 doi:10.20944/preprints201710.0119.v2

Article

Monitoring of Structures by a Laser Pointer. Dynamic Measurement of Rotations and Displacements of the Elastic Line of a Bridge: Methodology and First Test

Serena Artese [1,*], Vladimiro Achilli [2] and Raffaele Zinno [3]

[1] Dept. of Civil Engineering, University of Calabria, Via Bucci cubo 45B, 87036 Rende, Italy; E-Mail: serena.artese@unical.it
[2] Dept. of Civil, Environmental and Architectural Engineering, Via Marzolo, 9, 35131 Padova, Italy, E-Mail: vladimiro.achilli@unipd.it
[3] Dept. of Informatics, Modeling, Electronic and System Engineering, University of Calabria, Via P. Bucci cubo 42C, 87036 Rende, Italy; E-Mail: raffaele.zinno@unical.it
* Correspondence: serena.artese@unical.it; Tel.: +39-0984-496768

Abstract:
Deck inclination and vertical displacements are among the most important technical parameters to evaluate the health status of a bridge and to verify its bearing capacity. Several methods, both conventional and innovative, are used for structural rotations and displacement monitoring; no one of these does allow, at the same time, precision, automation, static and dynamic monitoring without using high cost instrumentation. The proposed system uses a common laser pointer and image processing. The elastic line inclination is measured by analyzing the single frames of a HD video of the laser beam imprint projected on a flat target. For the image processing, a code was developed in Matlab® that provides instantaneous rotation and displacement of a bridge, charged by a mobile load. An important feature is the synchronization of the load positioning, obtained by a GNSS receiver or by a video. After the calibration procedures, a test was carried out during the movements of a heavy truck maneuvering on a bridge. Data acquisition synchronization allowed to relate the position of the truck on the deck to inclination and displacements. The inclination of elastic line was obtained with a precision of 0.01 mrad. The results demonstrate the suitability of the method for dynamic load tests, control and monitoring of bridges.

Keywords: laser pointer, displacement monitoring, laser fingerprint, video, data synchronization.

1. Introduction

The possibility to perform fast and accurate image processing, thanks to the power of the most recent computers, allows us to conceive new exciting applications of this technology in several fields and, in particular, for the monitoring of large structures. The projection of the tangent to the elastic line of a girder, materialized by a light beam, on an image sensor or on a target can be effectively used for this purpose. Nowadays this is possible in a cheap and simple way, thanks to the laser technology. Several laser pointers, characterized by low cost, small dimensions and weight, low power, limited beam divergence and good pointing stability, are presently available on the market. All these characteristics allow the development of a technique for monitoring large structures and in particular bridges.

Inclinations and vertical displacements are among the most relevant technical parameters for assessing the health status of a bridge structure and for checking its load capacity. These parameters are also used to verify if the structural response of a bridge under various loading conditions is the one foreseen in the design phase. To control the state of health of a bridge before the opening to

traffic, the structure is usually charged by static loads, materialized by a convoy of heavy trucks parked on the deck in known positions. The deflections of the girders are then measured by using levels or total stations, while rotations are in general obtained by inclinometers. The Italian Rules for Constructions NTC 2008, e.g., impose a load test for every new bridge. Static tests, in relation to the importance of the work, can be supplemented by dynamic tests on structural elements [1].

Several methods, both conventional and innovative, are used for structural movement monitoring; all of these have pros and cons. (1) Dial gauges, often-used for measurements of floor slabs deflections, are difficult to install and manage, due to the height of bridges and to the presence of water; (2) Digital levels are characterized by high precision, but they cannot perform dynamic multitarget measurements; (3) Robotic total stations can perform 3D coordinates measurements with a sampling rate up to 7 Hz and for velocities up to about 10 cm/s [2-3]. The high precision and the automation of measurement can be joined to the possibility of data transfer over the internet and remote management [4], but the high cost of this high-end instruments limits their use for long-term bridge monitoring; (4) GNSS satellite-surveying are often used for long span bridges [5-8]. The attainable precision is high and the maximum sampling rate exceeds 20 Hz for the recent instruments. The main disadvantage is due to the mandatory antenna positioning on the point to measure; (5) Terrestrial laser scanning (TLS) is by now a consolidated technique for the surveying of bridges under static conditions [9-11]. The comparison of scans acquired at different times, allows us to obtain, e.g., the deviations between corresponding points of the bridge surface in different situations (loads, temperature, etc.). With regard to dynamic monitoring, the high sampling rate of line scanners, used in Mobile Mapping Systems, can be exploited. In particular, rotations and deflections of the superstructure of a bridge could be dynamically measured in near real time. One must consider that the best fitting line has in general a better accuracy than that of each single measured point, so the final result could reach a precision higher than that declared for the instrument used [9,12]; (6) Micro Electro-Mechanical Systems (MEMS) have been recently proposed for deflection measurement using inclination parameter measurements [13]. The results are affected by the high S/N ratio for dynamic tests; (7) Digital Image Correlation is a promising technique for bridge deflection measurements, also thanks to the increasing resolution of the last digital cameras [14-16].

The use of a laser beam for measuring deflections is by now a consolidated technique. A laser based displacement/deflection measurement system is described in [17]. In order to achieve a remote measurement, the laser beam of a digital level is collimated and directed to a detector array, which is attached to the remote object to be measured. The system is not suitable for long-term measurements, since the level and the array must be placed on the monitored object and these expensive instruments must be left unattended. Recently a concept of measuring devices using a laser diode and a CCD camera has been proposed for structural monitoring [18].

Among the several technologies used for structures dynamic displacement monitoring, the methods based on laser projection-sensing are increasingly being used, thanks to the availability of low-cost hardware. In this context, a methodology able to conjugate high precision, low cost and easiness of use has been developed. The measurement of the inclination is obtained by the variation of the tangent to the elastic line, materialized by the laser beam generated by a pointer attached to the deck bridge structure, and projected on a screen located at an adequate distance, in order to amplify the movement of the laser fingerprint and to get, therefore, a remarkable result accuracy. A video of the oscillations of the laser footprint during the monitoring activities is acquired. By analyzing the single frames, the variable position of the laser footprint centroid gives information about the inclination changes and, consequently, about the dynamic deflections. The position of the dynamic load can be detected by a video and/or GNSS positioning. The synchronization of acquisitions is performed by using GPS time.

The method is characterized by: (1) Moderate cost; (2) Low weight and small size hardware; (3) Ease of installation; (4) The precision requested for bridge deflection monitoring; (5) High frame rate (30 frames per second, upgradeable to 120 by using a common action camera).

Preprints (www.preprints.org) | NOT PEER-REVIEWED | Posted: 11 December 2017 doi:10.20944/preprints201710.0119.v2

A method for displacement monitoring by using a laser beam, a projection plate plane and a camera has been presented in [19]. The method described in the present paper differs mainly in the following aspects: (1) In our test, a common low-cost laser pointer, battery-powered, is used; (2) The lab tests described in [19], conducted on a bridge model, refer to loads in a fixed position, so the synchronization of load positioning and images capturing, that represents a fundamental topic for dynamic monitoring, is not considered; (3) Our test has been performed on a real bridge, with a real mobile load.

In the following, the methodology for monitoring of dynamic inclination and displacement of a bridge by using a low-cost laser pointer, characterized by low cost, ease of implementation and high precision, is presented. Another important characteristic of this methodology is the synchronization of the moving load position and of the inclination and deflection measurement. The experimental test carried out on a real bridge demonstrates the usability of this method for dynamic structures monitoring.

This paper covers: (1) the description of the methodology; (2) the hardware components (laser pointer, digital cameras, GNSS receiver, computer); (3) the software implemented (determination of laser footprint, time registration, inclination and displacement measurement); (4) the calibration procedures; (5) the in-field test; (6) the discussion of results.

2. Materials and Methods

2.1 The methodology

The proposed method takes advantage of the laser pointers' property to provide a steady pointing direction and produce a long-range, high-brightness visible imprint.

The footprint of a laser positioned at the intrados of a beam and projected on a plane target approximately orthogonal to the direction of the ray, will undergo a displacement ΔH due to two components: (1) the lowering or raising of the laser source and (2) the variation of the laser beam inclination. Both components are linked to the movements and inclinations of the structure to which the laser source is locked (Figure 1).

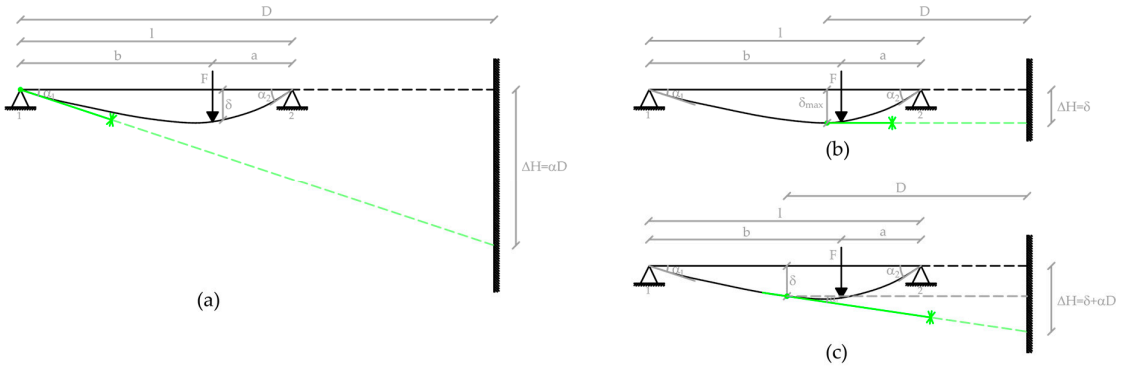

Figure 1. The displacement of the laser footprint in three cases: **(a)** laser fixed to a point subject only to inclination; **(b)** laser fixed to a point subject only to lowering; **(c)** laser fixed to a point with both inclination and lowering.

The component (1) produces a shift δ of the laser footprint equal to the displacement of the laser source. The component (2) causes a displacement αd proportional to the distance between the laser source and the target. It is therefore possible to greatly amplify this displacement by positioning the target at a convenient range; this allows obtaining the tilt variation with remarkable precision.

Lowering and inclination vary depending on the type of structure and on the point of application of the load [20]. E.g., in the case of a point load applied to a simply supported uniform cross-section

Preprints (www.preprints.org) | NOT PEER-REVIEWED | Posted: 11 December 2017 doi:10.20944/preprints201710.0119.v2

beam, that is the structural scheme used for most of the existing bridges, the maximum displacement is given by:

$$\delta_{max} = \frac{Fa(l^2 - a^2)^{3/2}}{9\sqrt{3}lEI} \quad (1)$$

This maximum deflection occurs at a distance x_1 from the closest support, given by:

$$x_1 = \sqrt{\frac{l^2 - a^2}{3}} \quad (2)$$

The slopes at the ends are:

$$\alpha_1 = \frac{Fa(l^2 - a^2)}{6lEI}$$
$$\alpha_2 = \frac{Fab(2l - a)}{6lEI} \quad (3)$$

where:

F = Force acting on the beam
l = Length of the beam between the supports
E = Modulus of Elasticity
I = Area moment of Inertia of cross-section
a = Distance from the load to the closest support (i.e. a ≤ l/2)

the ratio between maximum deflection and slope at end 1 is given by:

$$\frac{\delta_{max}}{\alpha_1} = \frac{2\sqrt{(l^2 - a^2)}}{3\sqrt{3}} \quad (4)$$

the ratio between the deflection at the distance x from the end and the slope at end 1 is given by:

$$\frac{\delta_x}{\alpha_1} = \frac{x\,(l^2 - x^2 - a^2)}{(l^2 - a^2)} \quad (5)$$

By measuring the inclination at an extreme point where the laser pointer is fixed and by knowing the point of application of a load, it is therefore possible to obtain the lowering of the span at any point, by using equation (5).
In the case of a different structural scheme, the relevant equations, easily findable in the civil engineering handbooks, should be used. The accuracy of the result depends on the correspondence between the as built and the structural scheme of the design.
The measurement of the slope due to a load is obtained by the variation of the tangent to the elastic line, materialized by the laser beam projected by the pointer, fixed to the truss beam of the bridge, on a screen located at a suitable distance, in order to amplify the movement of the laser fingerprint and to get, therefore, a remarkable result accuracy (see Figure 1a). A video of the oscillations of the laser footprint is acquired; by analyzing the single frames, the variable position of the laser footprint centroid (ΔH in Figure 1a) gives information about the slope (angle α) changes and, consequently, about the dynamic deflections. The position of the dynamic load can be detected by a video and/or GNSS positioning. The synchronization of the acquisitions is performed by using GPS time.
A first test was carried out on a bridge, whose structure is a simply supported space frame girder.

2.2 The hardware components

The hardware components are: (1) a laser pointer; (2) a digital camera for laser footprint video capturing and a camcorder for the video of the mobile load; (3) a GNSS receiver; (4) a computer with a synchronized clock.

 doi:10.20944/preprints201710.0119.v2

169 2.2.1 The Laser Pointer

170 A SCITOWER SCT306-532nm laser pointer was used. The main characteristics are resumed in
171 Table 1.

172 **Table 1.** Characteristics of the laser pointer.

Feature	Value
Wavelength	532 ± 0.1 nm (Green)
Beam diameter	2.0 mm
Beam divergence	0.8 mrad
Power	100 mW (Gaussian Beam)
Pointing stability	< 0.05 mrad
Beam spot roundness	≧ 90 %
Laser distance	～ 500 m
Warm-up time	≦ 1 minute
Lifetime	≧8000H

173

174 The laser pointer was mounted on a Newport Research Corporation model 810 laser mount,
175 provided with a strong magnetic base and two micrometric adjustment screws for a two axis
176 positioning.

177 2.2.2 The Digital Camera

178 The video of the laser footprint was acquired by using a NIKON D610 camera with a 55 mm
179 NIKKOR lens. The main characteristics are shown in Table 2.
180

181 **Table 2.** Characteristics of the NIKON D610 digital camera

Feature	Value
Type	Single-lens reflex digital camera
Effective pixels	24.3 million
Image sensor	Nikon FX format 35.9 x 24.0 mm - DX format 24x16 mm
File format	NEF (RAW), JPEG, NEF (RAW)+JPEG
Lens	NIKKOR 18-55mm f/3.5-5.6G VR
Shutter	Electronically-controlled vertical-travel focal-plane shutter
ISO sensitivity	ISO 100 to 6400 in steps of 1/3 or 1/2 EV
HD frame and frame rate	1,920 x 1,080 pixels; 30p (progressive), 25p, 24p

182

183 As for the video of the mobile load (a truck), a Canon Legria HF R78 Full HD Handycam was
184 used.

185 2.2.3 The GNSS Receiver

186 The GNSS receiver is an Ublox NEO-M8T provided with a cheap patch antenna. The NEO-M8T
187 is a timing receiver, but it can provide access to raw measurements on L1 (carrier-phase,
188 pseudorange, Doppler) for all available GNSS constellations and augmentation systems. For our
189 aims the receiver was configured to track GPS and GLONASS.

190 2.2.4 The Computer

191 A Dell XPS 13 9360 Notebook was used. The CPU is an Intel Core i7-7500U with a 2.7GHz clock
192 and 8 GB DDR SDRAM. The notebook is provided with a 256 GB SSD hard disk, a 13.3 inch Full HD

Preprints (www.preprints.org) | NOT PEER-REVIEWED | Posted: 11 December 2017 doi:10.20944/preprints201710.0119.v2

display and a graphic card Intel HD 620. The operating system is Windows 10 Pro. The synchronization with *time.windows.com* can be performed with an accuracy of 1 ms. Time format was set up in order to show hundredths of a second.

2.3 The software implemented

A program was developed in Matlab® for the determination of the laser footprint centroid projected on a flat target. The program uses the results of the calibration of the digital camera, described afterwards. With regard to the mean scale of the frame, the Ground Sample Distance (GSD) is obtained at the beginning of the shoot, given that a millimeter paper glued to a rigid plastic tablet is used as target. The millimeter paper allows to obtain the GSD, theoretically different for each pixel, but it has to be considered that the target is fixed vertically and the camera optical axis is horizontal, so the scale of the image in the vertical direction is practically identical in all the zones of the frame.

In order to obtain the position of the laser footprint centroid, for each frame, an intensity cut-off is performed preliminarily, which eliminates noises and the grid of the millimeter paper from the image. The centroid coordinates (row and column) are then calculated in pixels, through a weighted average: each pixel is assigned a weight equal to its intensity.

The row and the column of the centroid are:

$$row = \frac{\sum_{i=1}^{n}\sum_{j=1}^{m} I_{i,j}\, i}{m\, n} \tag{6}$$

$$col = \frac{\sum_{i=1}^{n}\sum_{j=1}^{m} I_{i,j}\, j}{m\, n} \tag{7}$$

where:

row= row coordinate of the centroid
col= column coordinate of the centroid
n = number of rows of the frame
m = number of columns of the frame
I = Intensity of the pixel

According with literature regarding image processing, the coordinates of the centroid can be obtained with an accuracy of .1 pixels [21]. For our aims, this accuracy is redundant, since the pointing instability is greater than one pixel.

The coordinates of centroid are then converted in mm, by using the known GSD.

If the camera settings provide a very low ISO sensitivity and a small diaphragm aperture, you can get a better defined shape of the laser beam footprint and avoid image saturation in the center zone of the footprint. This allows a more accurate determination of the centroid.

Since the position of the centroid is given for each frame, it is possible to evaluate the displacement of a monitored point with a sampling rate equal to the 30 Hz frame rate of the camera. Thus we obtain a graph of the centroid position as a function of time. Since the acquisitions of the video and of the moving load position are synchronized, the instantaneous displacement of the laser beam footprint is correlated to the position of the mobile load.

A module of the implemented software is devoted to the calculation of the deflection. In the first version, the laser pointer is considered fixed to an end of the bridge span; in this case the deflection of the laser footprint is due just to the variation of the inclination of the laser beam, since the end of the span has no deflection. Inputs of the module are: (1) the distance from the laser pointer to the target; (2) the section inertia properties of the bridge in case of non uniform cross-section beams; (3) the position of the mobile load acquired by the GNSS receiver.

Preprints (www.preprints.org) | NOT PEER-REVIEWED | Posted: 11 December 2017 doi:10.20944/preprints201710.0119.v2

Once obtained the slope of the laser beam, the deflection is computed in real time for a requested position, e.g. for the midspan and for uniform cross-section by using equation (5). The procedure is performed for each frame of the acquired video.

2.4 The calibration procedures

For the calibration of the camera, an upgrade of a well-known procedure [22, 23], developed using Matlab®, has been used. The procedure has been applied to the NIKON D610 camera with a 55 mm NIKKOR lens configured with a HD frame (1920 x 1080). A calibration plate with an accuracy of .1 mm has been used. Figure 2a shows the points of intersection automatically recognized by the software. If necessary, the operator can correct any errors or eliminate false positives identified by the automatic procedure. The main parameters of the tested camera are shown in Figure 2b. The results obtained are: focal length, principal point, skew, radial and tangential distortion parameters.

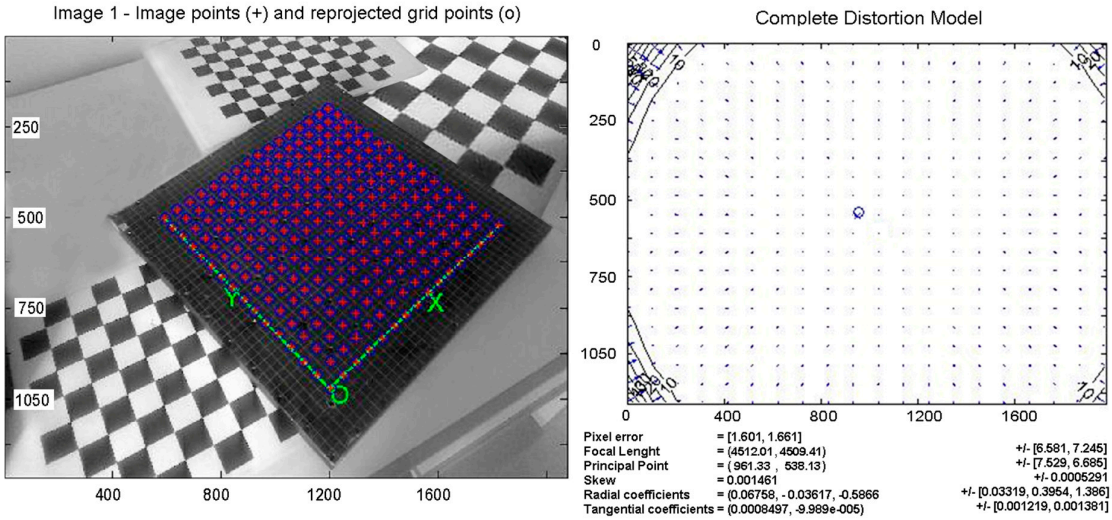

Figure 2. (**a**) The crosses of the calibration grid automatically recognized by the calibration software; (**b**) The distortion model of the calibrated camera. The coordinates and the results are in pixels.

After the camera calibration, to evaluate the accuracy of the centroid coordinates obtained by the aforementioned software, a lab test was carried out. The laser pointer was fixed to a linear motion system Impex HVP060 AM, characterized by a positioning precision of 0.03 mm.

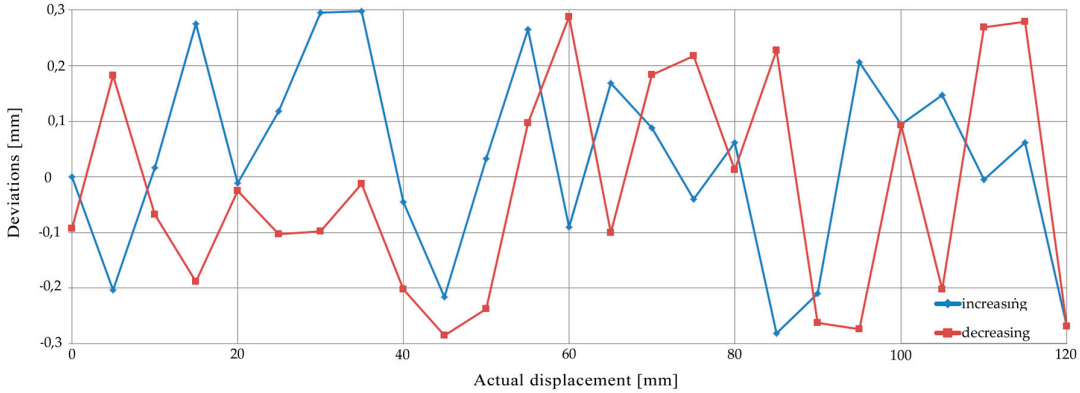

Figure 3. The deviations between the displacements obtained by the software and the from the displacements produced

The beam was projected orthogonally on a flat target and the laser pointer was shifted of 120 mm, with 5 mm steps, by means of the drive unit. Shifting was applied many times back and forth, thus resulting in loop processes. In Figure 3 the deviations between the displacements of the

Preprints (www.preprints.org) | NOT PEER-REVIEWED | Posted: 11 December 2017 doi:10.20944/preprints201710.0119.v2

centroid of laser footprint obtained by the software and the ones produced by the linear motion system are shown for a loop. The horizontal axis represents the displacement of the laser beam; the blue line represents the deviations during the increasing displacements, whereas the red line represents the deviations during the decreasing ones. The maximum deviation is 0.3 mm, while the standard deviation is 0.13 mm.

To verify the laser pointer stability, the pointer and the target were positioned on the bridge to be monitored, to have the same layout than the one of test to be carried out. Fifteen videos of five minutes were shot at an hour interval and, for each video, the oscillations of the laser fingerprint centroid were obtained. The short term instability was one fifth of the declared pointing stability: in fact, a maximum oscillation of 5 pixels during each video was measured, corresponding to an angle of about 0.01 mrad, whereas the maximum difference measured in all videos was 14 pixels.

3. The Test

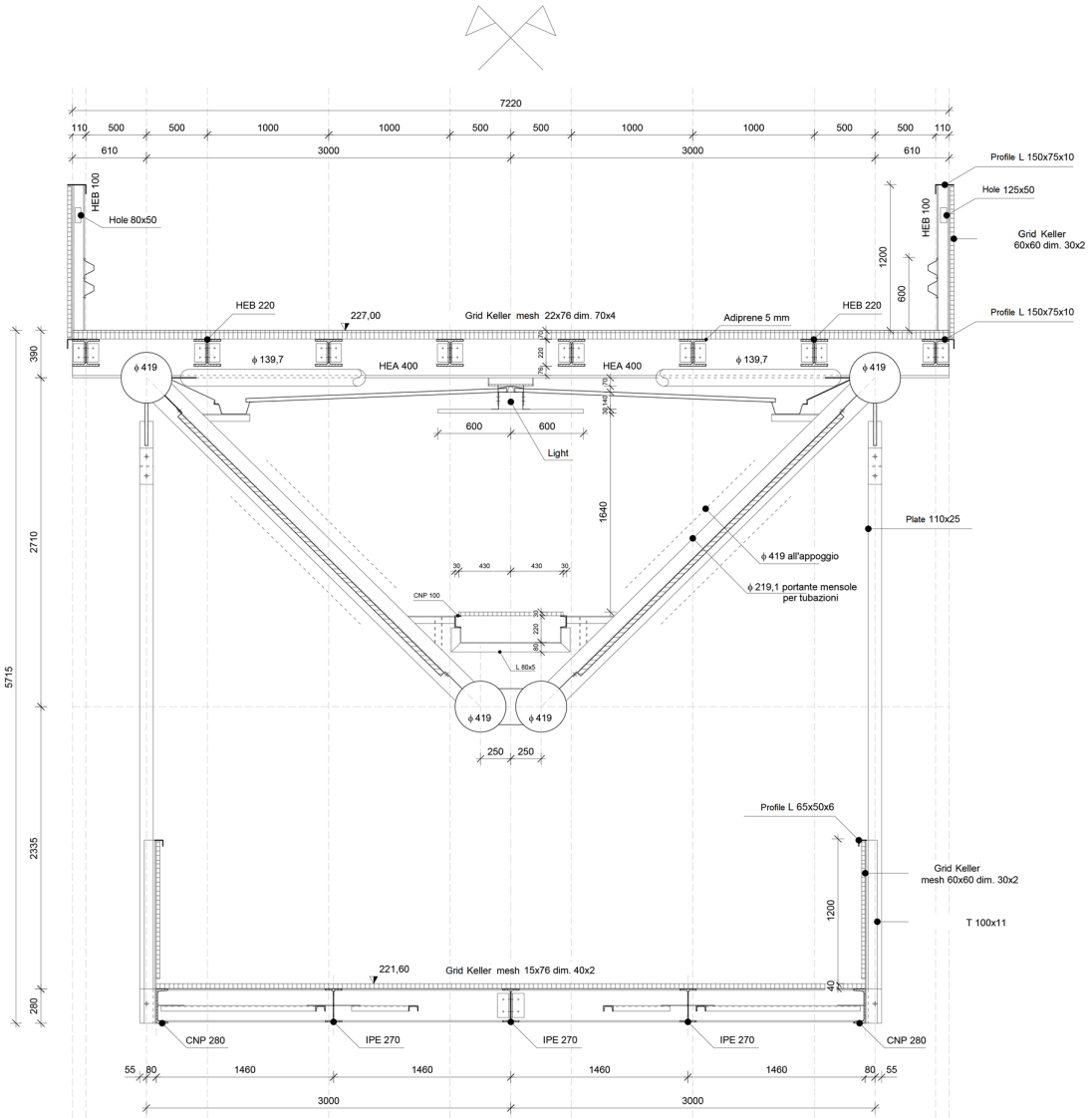

Figure 4. Cross section of the double-deck bridge at the University of Calabria.

The test was carried out on a bridge at the University of Calabria, Italy. The layout of the university is characterized by a South-North axis; all buildings are aligned to the sides of a central pathway

Preprints (www.preprints.org) | NOT PEER-REVIEWED | Posted: 11 December 2017 doi:10.20944/preprints201710.0119.v2

built partly on double deck bridges: the upper deck can be used for vehicular traffic, while the lower one is reserved for pedestrians (Figure 4).

The layout of the test is shown in figure 5. The laser pointer is fixed to a tubular element of the space frame girder of the bridge, close to the end of the span (Figure 6, 7). The laser beam is projected onto an A4 size flat target, fixed to a vertical wall of the north terminal abutment. If the free space beneath the bridge is less than 30 cm, the target can be fixed to any fixed position, e.g. to a cap of a pile, to a slope protection. To point exactly at the target, the pointer is mounted on a holder, usually used on optical tables, which allows precise horizontal and vertical movements. The holder is equipped with a strong magnetic base.

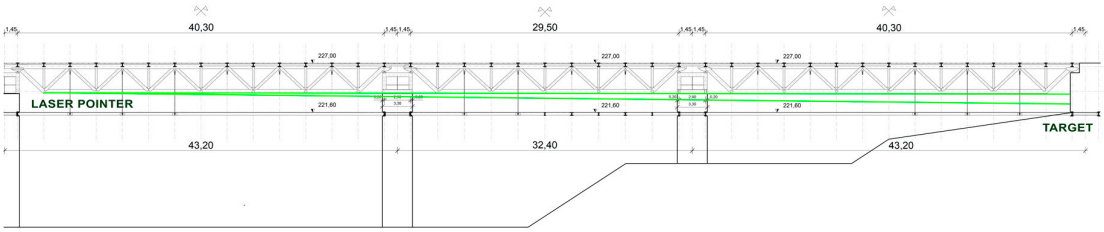

Figure 5. The layout of the test.

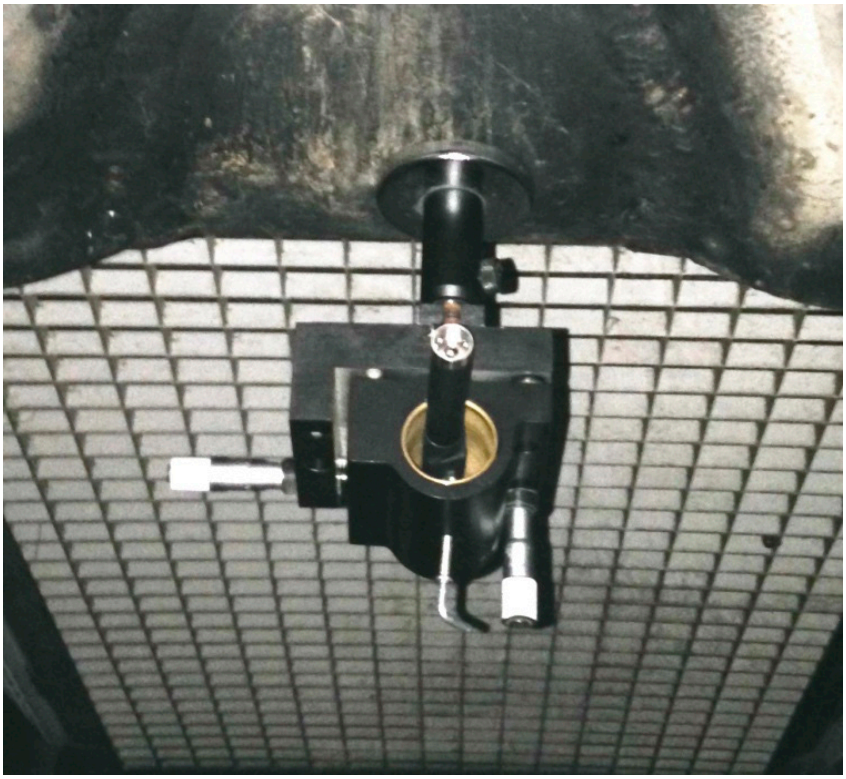

Figure 6. The laser pointer and the holder.

The NIKON 610 camera, used to obtain the footprint video, is positioned on a robust tripod, slightly lateral respect to the laser beam path. The camera-target distance is chosen in order to obtain a Field of View (FoV) slightly larger than the dimensions of the target. Due to the camera–target distance and the lens focal length, the mean GSD is 0.25 mm. Taking into account the pointing stability of the laser pointer, a smaller GSD would be useless. Given that the distance from the laser pointer to the target is 115.70 m, we obtain a beam footprint diameter of 95 mm and a maximum theoretical pointing instability of 5.8 mm (23 pixels), taking into account the characteristics of the

 doi:10.20944/preprints201710.0119.v2

Table 1. This suggests that the method can achieve good results even for shorter pointer to target distances.

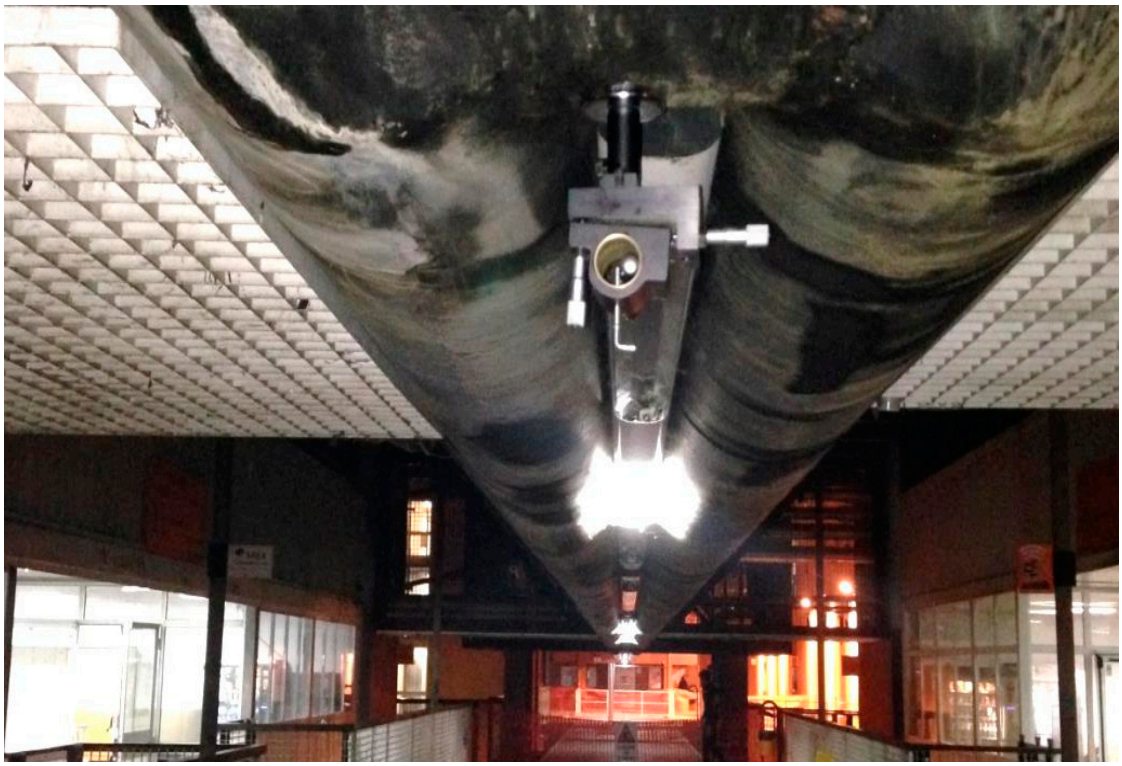

Figure 7. The pedestrian deck: the target is on the front wall.

The projection plate plane and the optical path are not angled. Actually, by using e.g. a 30° angle between laser beam and target plane like in [19], the movement of the laser spot centroid in the video image is amplified, and the measurement accuracy is theoretically increased, but this improvement is counterbalanced by the need to double the FoV and, consequently, the GSD.

The used technique allows us to determine the centroid of the footprint with an accuracy less than one pixel, thus the expected error in the measurements of the beam inclination is almost completely due to the laser pointer instability and can be conservatively evaluated 0.05 mrad.

The test was carried out during the movements of a truck elevator, used for work on the façade of a building alongside the bridge (Figure 8). The patch antenna of the Ublox NEO-M8T receiver was positioned on the cab roof. The weight of the truck was about 260 kN. The video of the mobile load was shot with the camcorder when the truck left the bridge. Due to the limited space, the truck performed some forward and backward movements along the left span to reach the optimal alignment before the final reverse running at a speed of about 4 m/s.

With regard to time synchronization, the Nikon 610 camera is provided with a GP-1 unit, an accessory that can provide the Coordinated Universal Time (UTC). For the synchronization of the camcorder, the display of the notebook, showing the GPS time rounded to the hundredths of a second, was framed before and after the video shot. In this way, the video's timing synchronization was obtained with an approximation equal to its frame rate of 30 fps.

Preprints (www.preprints.org) | NOT PEER-REVIEWED | Posted: 11 December 2017 doi:10.20944/preprints201710.0119.v2

Figure 8. The truck elevator on the upper deck of the bridge.

A frame of the video is shown in Figure 9. The image shows the truck during the backward running. The transverse beams of the upper deck, positioned every three meters, allow to determine the position of the wheels in the longitudinal direction. The origin of abscissae (positive in North direction) is fixed at the south end of the span.

The accurate abscissae of the truck were obtained by a cinematic differential positioning. The Ublox GNSS receiver was set to acquire data with a 5 Hz sampling rate, while the fixed GNSS station at University of Calabria was used as base. Furthermore, two points on transverse beams of the upper deck were surveyed previously, in order to perform a coordinate transformation and obtain the abscissae in the local reference system.

Figure 9. A frame of the camcorder video with the truck leaving the bridge. The transverse beams on the deck are used to obtain the position in the direction parallel to the longitudinal axis of the bridge.

 doi:10.20944/preprints201710.0119.v2

4. Results and Discussion

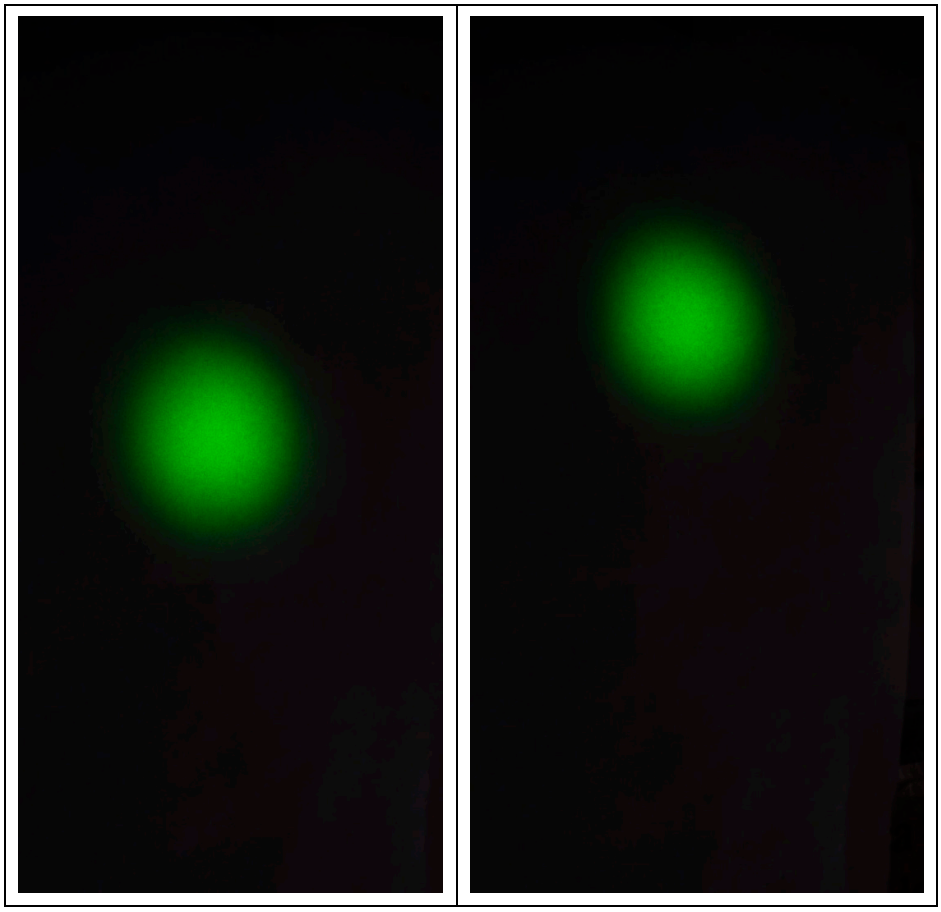

Figure **10**: Two frames acquired at the beginning and at the end of the test: after the truck left the bridge, the footprint is higher.

In Figure 10 we can observe two frames obtained at the beginning and at the end of the test. The ISO sensitivity and the aperture were chosen in order to obtain a radiometric cut off, thus achieving two goals: a better defined shape of the laser beam footprint was obtained and the saturation of the image in the center zone of the footprint avoided. This allows a more accurate determination of the centroid. The frames were processed by using the code in Matlab® previously described and the dynamic position of the centroids in pixel coordinates (rows, columns) was obtained.

In Figure 11, the height of the centroid during the test is shown. In red a trend line (30-sample moving average) is drawn. The origin of ordinates is at the bottom of the frame and the values have been transformed from pixels into mm, while the scale of the frames has been obtained by using the known GSD. Abscissae are in seconds.

It is possible to observe that the pointing stability was less than 0.05 mrad (corresponding to 5.8 mm for the pointer–target distance equal to 115.70 m).

From a qualitative point of view we can observe that the forward – backward movements of the truck are clearly reflected in the movements of the laser beam. Furthermore, some damped oscillations are recognizable after the truck left the bridge.

Preprints (www.preprints.org) | NOT PEER-REVIEWED | Posted: 11 December 2017 doi:10.20944/preprints201710.0119.v2

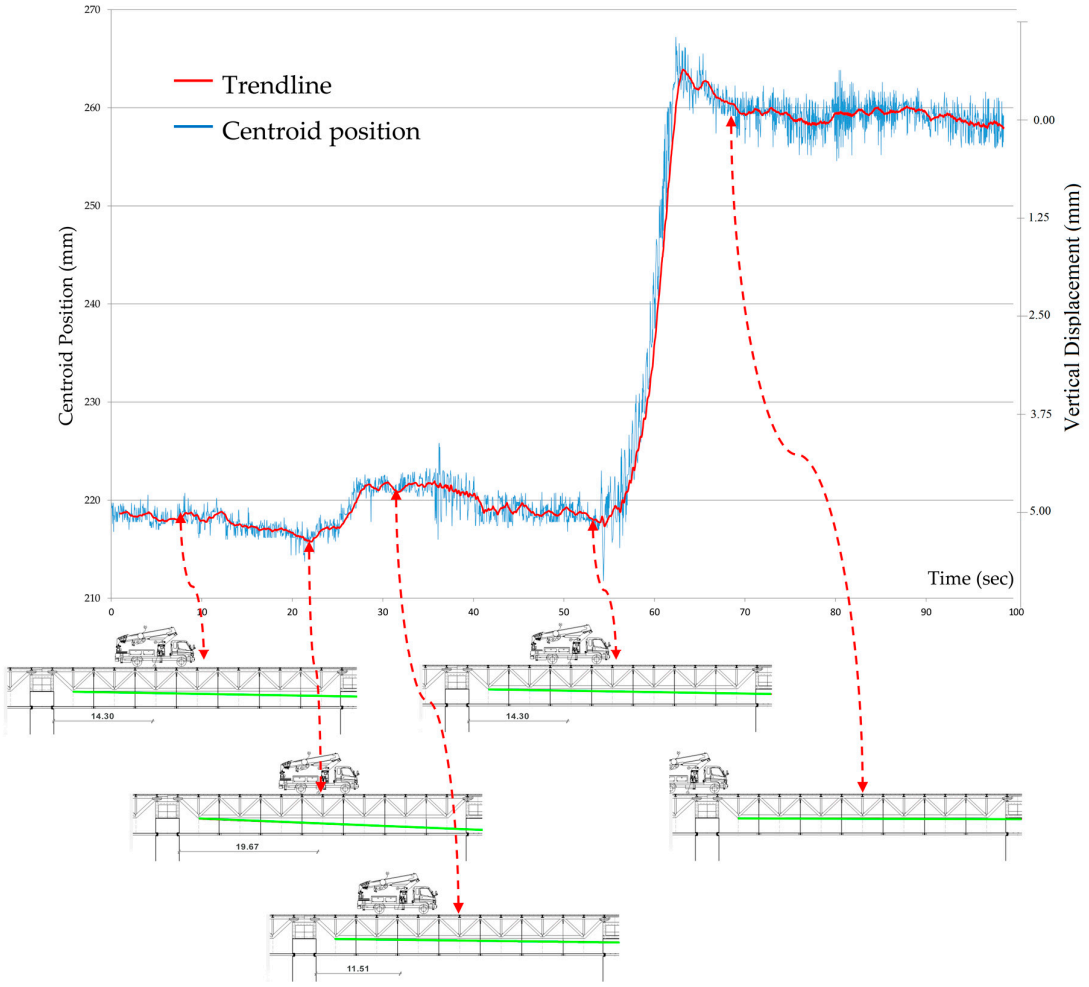

Figure 11: The vertical position of the centroid of the footprint during the test.

As regards the truck position, the abscissae (previously defined and shown in Figure 9) obtained by using the GNSS positioning were used for the elaborations. A comparison between the abscissae obtained by the camcorder video and by the GNSS solution showed a maximum deviation of 0.3 m.

The span of the bridge is 40.30 m, while the barycenter of the truck, at the beginning of the test, is at 14.30 m from the bearing.

After 55 seconds from the beginning of the video, a sudden variation is evident, equal to about 40 mm, corresponding to an inclination change of 0.346 mrad. Given that the laser is positioned very close to the bearing and the section inertia properties of the truss beam are constant, the estimation of the maximum deflection can be made by using equation (4). The variation of the maximum truss beam deflection obtained this way is 5.0 mm. The variation of the deflection in the midspan, obtained by using equation (5), is 4.9 mm.

A more accurate evaluation was performed by using a FEM code, written at University of Calabria [24]. The obtained deflection was 4.8 mm.

A precise measurement was done by using a Leica 1201+ total station. The axis of a bolt of a steel connection in the midspan was used as a target and its position was surveyed before and after the test. The measured variation of the truss beam deflection was 4.8 mm, 2% less than the result obtained with the proposed methodology.

The use of the positions obtained by the camcorder video and by the GNSS solution gave comparable results, with differences less than 5%. Both techniques have pros and cons. GNSS allows to obtain more accurate positioning along with a simple and accurate time synchronization, but a receiver must be installed on the vehicle. The video gives less accurate positioning, implies more computer processing both for images and time synchronization, but it can be used also for non instrumented vehicles. For official load tests, the first technique is the most suitable; in fact, in order to obtain the requested precision of positioning, the vehicles used as mobile loads can be easily provided with a GNSS receiver. For the monitoring of a bridge under normal conditions, instead, the second technique is the only currently usable.

5. Conclusions

In the light of the results of the test carried out on a real case, we can conclude that the method proposed allows to obtain the rotations of a bridge with the precision required for load tests and monitoring. The low cost of the components and the ease of configuration make the method a suitable alternative to the traditional methods. Its reliability has been demonstrated both from a qualitative and quantitative point of view. The forward – backward movements of the truck used for the experimental test are clearly reflected in the movements of the laser beam. For the bridges with simply supported uniform cross-section beam, that represent most of the existing bridges**,** the displacements can be estimated with a good accuracy. In our test, the deviation between the beam deflection obtained with the described method and the one measured by a high-end total station was about 2%.

Along with the precision obtained, a noticeable goal is the synchronization of the acquisitions, that allows to get the instantaneous position of the mobile load and the deflection.

In the next future, the use of a camera with high frame rate is foreseen, to demonstrate the usefulness of the method for the control of the bridge's natural frequencies.

Author Contributions: Serena Artese conceived the methodology. Serena Artese and Vladimiro Achilli designed the experiments. Raffaele Zinno analyzed the data. All the authors performed the experiments and prepared the manuscript.

Conflicts of Interest: The authors declare no conflict of interest.

References

1. Italian Ministry of Infrastructures and Transportations. NTC (2008). Norme Tecniche per le Costruzioni, Ministerial Decree 14/01/2008, Official Gazette n. 29, Rome, Italy, 2008.
2. Lienhart, W.; Ehrhart, M.; Grick, M. High frequent total station measurements for the monitoring of bridge vibrations. *Journal of Applied Geodesy* **2017**, *11*, 1-8, doi: 10.1515/jag-2016-0028
3. Yu, J.; Zhu, P.; Xu, B.; & Meng, X. Experimental assessment of high sampling-rate robotic total station for monitoring bridge dynamic responses. *Measurement* **2017**, *104*, 60-69, doi: 10.1016/j.measurement.2017.03.014
4. Artese, G.; Perrelli, M.; Artese, S.; Manieri, F. Geomatics activities for monitoring the large landslide of Maierato, Italy. *Applied Geomatics* **2014**, *7*, 171-188, doi: 10.1007/s12518-014-0146-8.
5. Lovse, J. W.; Teskey, W. F.; Lachapelle, G.; & Cannon, M. E. Dynamic deformation monitoring of tall structure using GPS technology. *Journal of surveying engineering* **1995**, *121(1)*, 35-40, doi: 10.1061/(ASCE)0733-9453(1995)121:1(35).
6. Roberts, G.; Meng, X.; Dodson, A. Integrating a Global Positioning System and Accelerometers to Monitor the Deflection of Bridges. *Journal of Surveying Engineering* **2004**, *130*, 65-72, doi: 10.1061/(ASCE)0733-9453(2004)130:2(65).
7. Yu, J.; Meng, X.; Shao, X.; Yan, B.; Yang, L. Identification of dynamic displacements and modal frequencies of a medium-span suspension bridge using multimode GNSS processing. *Engineering Structures* **2014**, *81*, 432-443, doi: 10.1016/j.engstruct.2014.10.010.
8. Yu, J.; Yan, B.; Meng, X.; Shao, X. Measurement of bridge dynamic responses using network-based real-time kinematic GNSS technique. *Journal of Surveying Engineering* **2016,** 142(3), doi: 10.1061/(ASCE)SU.1943-5428.0000167.

9. Gordon, S.; Lichti, D. Modeling Terrestrial Laser Scanner Data for Precise Structural Deformation Measurement. *Journal of Surveying Engineering* **2007**, *133*, 72-80, doi: 10.1061/(ASCE)0733-9453(2007)133:2(72).
10. Park, H. S.; Lee, H. M.; Adeli, H.; & Lee, I. A new approach for health monitoring of structures: terrestrial laser scanning. *Computer-Aided Civil and Infrastructure Engineering* **2007**, *22(1)*, 19-30, doi: 10.1111/j.1467- 8667.2006.00466.x.
11. Truong-Hong, L.; Laefer, D. F. Using Terrestrial Laser Scanning for Dynamic Bridge Deflection Measurement, Proceedings of the IABSE Istanbul Bridge Conference, Istanbul, Turkey, 11-13 August 2014.
12. Artese, S. Survey, diagnosis and monitoring of structures and land using geomatics techniques: theoretical and experimental aspects. In *Geomatics research 2016*, Vettore, A., Ed.; AUTeC, Italy, 2017; pp. 31-42, ISBN 978-88-905917-9-2.
13. Yu, Y.; Liu, H.; Li, D.; Mao, X.; & Ou, J. Bridge deflection measurement using wireless mems inclination sensor systems. *International Journal on Smart Sensing & Intelligent Systems* **2013**, *6(1)*, 38-57, doi: 10.1.1.658.8791.
14. Yoneyama, S.; Ueda, H. Bridge deflection measurement using digital image correlation with camera movement correction. *Materials Transactions* **2012**, *53(2)*, 285-290, doi: 10.2320/matertrans.I-M2011843.
15. Kwak, E.; Detchev, I.; Habib, A.; El-Badry, M.; Hughes, C. Precise photogrammetric reconstruction using model-based image fitting for 3D beam deformation monitoring. *Journal of Surveying Engineering* **2013**, *139(3)*, doi: 143-155, 10.1061/(ASCE)SU.1943-5428.0000105.
16. Lu, W.; Cui, Y.; Teng, J. Structural displacement and strain monitoring based on the edge detection operator. *Advances in Structural Engineering* **2016**, *20*, 191-201, doi: 10.1177/1369433216660220.
17. Tang, C.; Li, E. The design of a laser-based digital displacement/deflection measurement system of a remote object and its calibration. Proc. SPIE 6829, Advanced Materials and Devices for Sensing and Imaging III, 68291T (24 January 2008); doi: 10.1117/12.757617.
18. Wilczyńska, I.; & Ćmielewski, K. Modern measurements techniques in structural monitoring on example of ceiling beams. Proceedings of 3rd Joint International Symposium on Deformation Monitoring (JISDM), Vienna, Austria, 30 March - 1 April 2017.
19. Zhao, X.; Liu, H.; Yu, Y.; Xu, X.; Hu, W.; Li, M.; Ou, J. Bridge displacement monitoring method based on laser projection-sensing technology. *Sensors* **2015**, *15(4)*, 8444-8463, doi: 10.3390/s150408444.
20. Chen, W.; Lui, E. *Handbook of structural engineering*, 2nd ed.; CRC Press: Boca Raton, United States, 2005; pp 1768, ISBN: 9780849315695.
21. Fisher, R. B.; Naidu, D. K. A Comparison of Algorithms for Subpixel Peak Detection. in J. Sanz (ed.), *Advances in Image Processing, Multimedia and Machine Vision*, Springer-Verlag, 1996, 385-404
22. Zhang, Z. A flexible new technique for camera calibration. *IEEE Transactions on Pattern Analysis and Machine Intelligence* **2000**, *22*, 1330-1334, doi: 10.1109/34.888718.
23. Artese, G.; Perrelli, M.; Artese, S.; Meduri, S.; Brogno, N. POIS, a Low Cost Tilt and Position Sensor: Design and First Tests. *Sensors* **2015**, *15*, 10806-10824, doi: 10.3390/s150510806.
24. Madeo, A.; Casciaro, R.; Zagari, G.; Zinno, R.; Zucco, G. A mixed isostatic 16 dof quadrilateral membrane element with drilling rotations, based on Airy stresses. *Finite Elements in Analysis and Design* 2014, 89, 52–66, https://doi.org/10.1016/j.finel.2014.05.013.